RSC Advances

PAPER

View Article Online
View Journal | View Issue

Cite this: *RSC Adv.*, 2023, **13**, 14580

Antioxidant activity of novel nitrogen scaffold with docking investigation and correlation of DFT stimulation†

Mona A. Shalaby,[a] Asmaa M. Fahim *[b] and Sameh A. Rizk[a]

Heterocyclic scaffolds are frequently employed in drug development to treat a variety of conditions, including cancers. These substances have the ability to engage covalently or non-covalently with particular residues in the target proteins, inhibiting them. In this study, the formation of N-, S-, and O-containing heterocycles by the interaction of chalcone with nitrogen-containing nucleophiles such as hydrazine, hydroxyl amine, guanidine, urea, and aminothiourea was explored. FT-IR, UV-visible, NMR, and mass spectrometric studies were used to confirm the heterocyclic compounds that were produced. These substances were tested for their antioxidant activity by their capacity to scavenge the artificial radicals 2,2-diphenyl-1-picrylhydrazyl (DPPH). The strongest antioxidant activity was demonstrated by compound **3** (IC_{50} = 93.4 μM), whereas compound 8 (IC_{50} = 448.70 μM) had the lowest activity when compared to vitamin C (IC_{50} 141.9 μM). Also, the experimental findings and the docking estimation of these heterocyclic compounds with **PDBID:3RP8** were in agreement. Additionally, the compounds' global reactivity characteristics, such as HOMO–LUMO gaps, electronic hardness, chemical potential, electrophilicity index, and Mulliken charges, were identified using DFT/B3LYP/6-31G(d,p) basis sets. The two chemicals that displayed the best antioxidant activity also had their molecular electrostatic potential (MEP) ascertained using DFT simulations.

Received 11th April 2023
Accepted 2nd May 2023

DOI: 10.1039/d3ra02393a

rsc.li/rsc-advances

1. Introduction

Heterocycles are extremely important in organic chemistry because they have so many uses in the biological, chemical, and medicinal sciences.[1–4] Organic heterocycle refers to cyclic organic compounds containing one or more hetero-atoms, including nitrogen, oxygen, sulfur, *etc.*[5–8] Different heterocyclic substances are essential to nature, medicine, and innovation. Moreover, these ring structures serve as the fundamental structural elements of a large number of biological molecules, including haemoglobin, DNA, RNA, vitamins, hormones, *etc.* Many medications that the FDA has approved for the treatment of various disorders also contain this structure.[9–12] A number of N-containing heterocycles with distinct properties and uses have recently gained popularity in the fields of chemical, pharmaceutical, and medical chemistry.[13–16] The heterocyclic nitrogen compounds such as pyrazole, pyrimidine, pyrazoline, and isoxazoline have shown high biological evaluation as Epirizole used as anti-inflammatory drug,[17,18] Dasatinib used to treat leukemia, [18]and Trimethoprim used as antibiotics.[19] Pyrazoline serves as a vital backbone in the development of new anticancer treatment agents, with several already being utilized clinically and others in ongoing research studies. By combining pyrazoline with alternative heterocyclic structures, there is potential to decrease adverse effects and combat drug resistance, making it an essential component in the design of efficient and secure cancer treatments.[20] Moreover, pyridines are important building blocks in pharmaceuticals due to their analgesic, anti-inflammatory, antitumor, and antiviral properties.[21]

Likewise, the O-containing heterocycles display a variety of pharmacological properties, including antibacterial, anti-HIV, anti-malaria, anti-cancer, anti-tubercular, and diabetic properties.[22–26] The iso-oxazolines exhibit antibacterial, antifungal, anticancer, and anti-inflammatory properties.[27] Furthermore, S-containing heterocyclic compounds are used in dyes, medicines, and agrochemicals as well as being key components of primary (cystine and methionine amino acids) and secondary metabolites (biotin and thiamine).[28,29] Benzothiazepines are recognized for their impact on cardiovascular functioning by acting as calcium channel inhibitors, and they have also been found to exhibit anticonvulsant and anticancer properties.[30] Antioxidants, either enzymatic or non-enzymatic, can prevent or reduce cellular damage caused by free radicals, unstable molecules generated by the body as a response to

[a]*Chemistry Department, Faculty of Science, Ain Shams University, Abbassia, P.O. 11566, Cairo, Egypt*

[b]*Green Chemistry Department, National Research Centre, Dokki, P.O. Box 12622, Cairo, Egypt. E-mail: asmaamahmoud8521@gmail.com*

† Electronic supplementary information (ESI) available. See DOI: https://doi.org/10.1039/d3ra02393a

environmental or other pressures.[31,32] The radical scavengers are molecules that play an important role in chemistry, biology, and material science. For example, they are used in food storage, pharmaceuticals, cosmetics, petroleum products, oil, rubber, and electronic device application.[33–37] Recently, it has been increasingly important to develop new radical scavengers with applications for industry and pharmaceuticals.[38–40] Microwave (MW) irradiation is a very useful tool in organic synthesis, where the required reaction times for the formation of the target compounds in synthetic organic chemistry are shorter compared to the conventional heating method.[41]

In this elucidation we synthesized different N-, S-, and O-containing heterocycles from the 2′-hydroxychalcone compound and analyzed them through spectral analysis such as FT-IR, mass, and NMR. The synthesized compounds were examined through scavenger radical inhibition as antioxidant activity using DPPH. Docking analysis of these compounds were evaluated through **PDBID:3RP8** and it was found that they exhibited a strong correlation interaction with hydrogen bond interaction. Furthermore, the DFT analysis of these heterocyclic compounds showed computability of their physical descriptors and its HOMO–LUMO analysis.

2. Results and discussion

2.1. Chemistry

We examined the reactivity of chalcone **1** towards aza-Michael addition reactions using different nitrogen-attacking nucleophiles (Michael donors) such as hydrazine hydrate, phenyl hydrazine derivatives, hydroxylamine, guanidine, urea, thiourea, and heterocyclic amines to form different heterocyclic active compounds. Different pyrazolines **3** and **4** were formed under microwave radiation from the reaction of chalcone **1** with hydrazine hydrate **2** in different solvents such as ethanol and acetic acid as the reported method[42,43] (Scheme 1). The IR spectrum of compound **3** showed characteristic stretching bands at 3339, 3006, and 1619 cm^{-1} due to NH, aromatic C–H, and C=N groups, respectively. Whereas compound **4**, the IR spectrum showed bands at 3032, 1615, and 1648 cm^{-1} due to aromatic C–H, and C=N, and C=O group, respectively. The two compounds **3** and **4** were supported the ABX system of pyrazoline ring protons and showed in ^{1}H-NMR at δ 2.94 and 3.21 ppm for H_A resonated as a pair of doublets of doublets, while for H_B appeared at δ 3.56 and 3.90 ppm as a pair of doublets of doublets, respectively. The H_X in the pyrazoline ring for compounds **3** and **4** appeared as a doublet of triplets or doublet of doublets at δ 4.79 and 5.44 ppm, respectively. The D_2O exchangeable singlet peak of OH appeared at 12.38 and 10.20 ppm for compounds **3** and **4**, respectively, while the NH proton for compound **3** appeared at 7.80 ppm. All the other aromatic protons were observed with their expected chemical shifts. Moreover, the formations of pyrazolines **6a–c** were synthesized *via* condensation reaction of chalcone **1** with different phenyl hydrazine derivatives **5a–c** as displayed in Scheme 1. The IR spectrum of pyrazoline rings of **6a–c** showed a characteristic bands at 1616, 1620, and 1615 cm^{-1} due to C=N group, also the ^{1}HNMR of ABX structure of pyrazoline ring protons for compounds **6a–c**. The signals for compounds **6a–c** appeared, respectively, at δ 3.21, 3.33, and 3.19 ppm for H_A resonated as a pair of doublets of doublets, while for H_B appeared as a pair of doublets of doublets at δ 4.01, 4.08, and 3.98 ppm, respectively. Also, The H_X in the pyrazoline ring for compounds **6a–c** appeared as a doublet of doublets at δ 5.40, 5.65, and 5.35 ppm, respectively. The D_2O exchangeable singlet peak of OH appeared at 10.55, 10.22 and 10.58 ppm for compounds **6a–c**, respectively. All the remaining aromatic protons were observed with their expected chemical shifts.

Furthermore, different varieties of condition reactions of chalcone **1** with hydroxylamine hydrochloride **7** were examined either with sodium acetate in ethanol, or sodium hydroxide as a base medium instead of using pyridine as previously reported[44] (Scheme 2). The reaction of chalcone **1** with hydroxylamine hydrochloride and sodium acetate in ethanol formed oxime **8** and didn't form the isoxazoline **9**. The method with sodium acetate using microwave afforded oxime **8** as the only product for the reaction. The IR spectra of compound **8** showed bands at 3321, 3028, and 1635 cm^{-1} due to OH, aromatic C–H, and C=N groups, respectively. The ^{1}H NMR supported the structure identity due to the appearance of the double bond

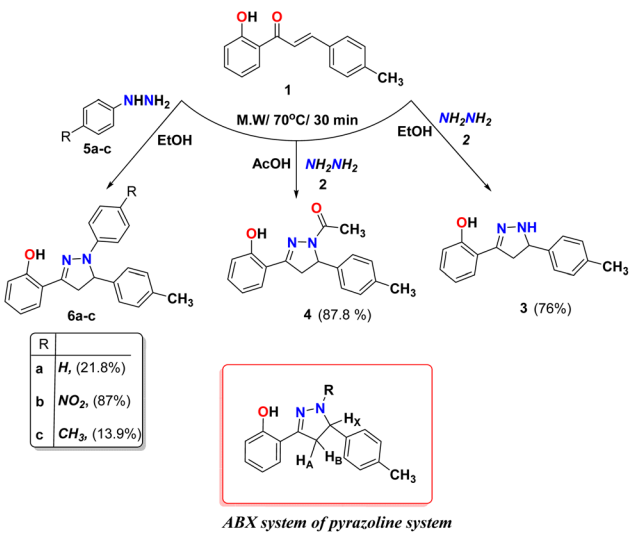

Scheme 1 Reaction of chalcone **1** with hydrazine hydrate in different condition and chalcone **1** with phenyl hydrazine derivatives.

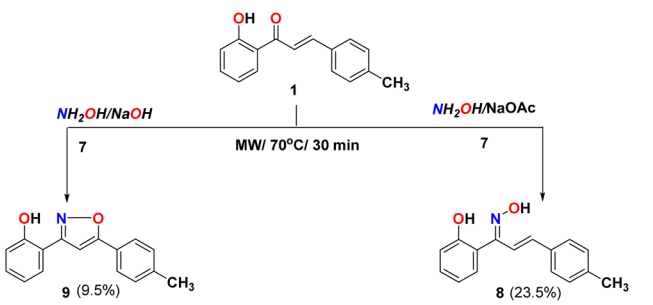

Scheme 2 Reactivity of chalcone **1** with NH_2OH in different basic condition.

peaks (J = 16.8 Hz) at 6.42 and 7.50 ppm revealed the pure geometrical with trans-configuration in addition to the D_2O exchangeable singlet peak of two OH at 9.65 and 11.35 ppm. While the reaction in presence of NaOH as a base afforded the isoxazoline **9**. Their IR spectra showed bands at 3281, 3028, and 1635 cm^{-1} due to OH, aromatic C–H, and C=N groups, respectively. The NMR supported the structure identity (*cf.* experimental part).

The reaction of chalcone **1** with guanidine **10** in the presence of KOH as a base gave the amino pyrimidine **11**, as shown in Scheme 3. This reaction was reported using *t*-BuOK as a base and 2-propanol as a solvent.[45] The IR spectra of amino pyrimidine **11** showed bands at 3356, 3259, 3089, and 1672 cm^{-1} due to OH, NH, aromatic C–H, and C=N groups, respectively. The ^{1}H NMR for compound **11** showed singlet peaks at 7.17, 7.80, and 14.03 ppm due to NH, CH pyrimidine ring, and OH, respectively. While the reaction of chalcone **1** with urea did not produce the expected compound pyrimidine and gave triaryl-5*H*-chromeno[4,3-*b*]pyridine **13**[46] and confirmed *via* spectral analysis such as FT-IR spectra that shows bands at 3053 and 1600 cm^{-1} due to aromatic C–H, and C=N groups, respectively. The ^{1}HNMR of compound **13** showed three singlet peaks appeared at 6.44, 8.10, and 13.80 ppm due to CH of the chromene ring, CH of the pyridine ring, and OH, respectively. Also, condensation of chalcone **1** with thiourea **14** gave the dimer product thiopyrimidine compound **15**, which was detected with the IR that shows bands at 3019 and 1613 cm^{-1} due to aromatic C–H, and C=N groups; respectively. The ^{1}H NMR for thiopyrimidine **15** showed one singlet peak at 8.52 ppm due to the CH of pyrimidine ring as showed in Scheme 3.

The cyclocondensation of chalcone **1** with 1,2,4-triazol-3-amine **16**, as shown in Scheme 4 in DMF gave the 2-(7-(*p*-tolyl)-[1,2,4]triazolo[1,5-*a*]pyrimidin-5-yl)phenol **17**. The IR for compound **17** showed bands at 3496 and 1687 cm^{-1} due to OH and C=N groups and the ^{1}H NMR showed singlet peaks at 8.72, and 12.38 ppm due to CH pyrimidine ring and OH, respectively. While the reaction of chalcone **1** with 2-amino-1*H*-imidazole-4,5-dicarbonitrile **18** in DMF as solvent afforded the corresponding 7-(2-hydroxyphenyl)-5-(*p*-tolyl)imidazo [1,2-*a*] pyrimidine-2,3-dicarbonitrile **19** and confirmed through spectral analysis such as FT-IR spectra that showed bands at 3493,

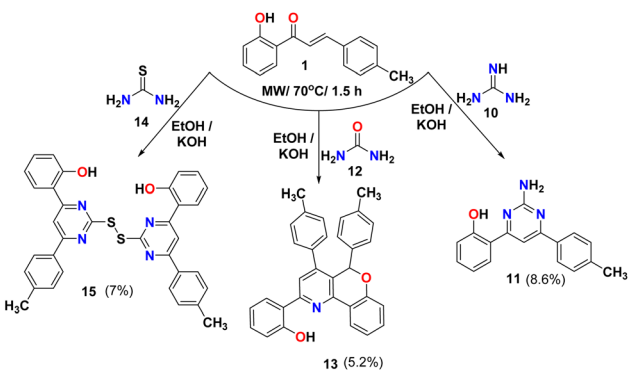

Scheme 3 Reaction of chalcone **1** with guanidine, urea, and thiourea.

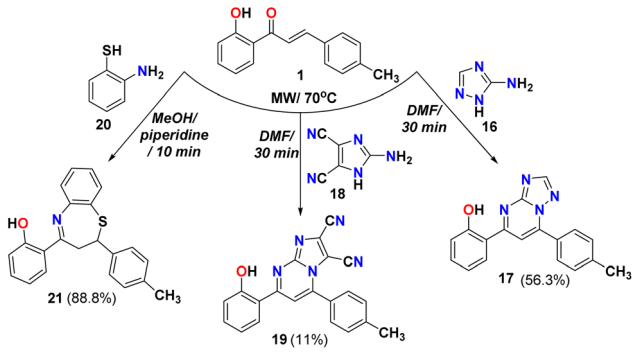

Scheme 4 Reactivity of chalcone **1** with amino-heterocyclic derivatives.

2246 and 1614 cm^{-1} due to OH, CN, and C=N groups; respectively. The ^{1}H NMR showed three singlet peaks appeared at 8.14, and 11.68 ppm due to CH of the pyrimidine ring, and OH, respectively. Furthermore, the Michael addition reaction of *o*-aminothiophenol **20** with chalcone **1** followed by cyclo-condensation to give the desired 1,5-benzothiazepine **21**. The same reaction was reported using *N*-methylimidazolium nitrate as a catalyst.[47] The IR spectra showed characteristic bands at 3428, 3051, 1598 cm^{-1} due to OH, aromatic C–H, and C=N double bond in the seven-membered ring heterocycle. The ^{1}H NMR of benzothiazepine **21** supported the ABX system where it showed a triplet at δ 2.90 ppm for H_A and two doublets of doublet at δ 3.50 and 5.22 ppm for the H_B and H_X; respectively. The mass spectrum exhibited a peak at m/z 345 attributable to the molecular ion as displayed in Scheme 4.

2.2. Antioxidant activities

The radical scavenging properties of compounds **3**, **4**, **6a–c**, **8**, **9**, **11**, **13**, **15**, **17**, **19**, and **21** were studied using a DPPH assay in methanol, whereby DPPH free radicals change their color from purple to yellow upon the quenching of the radical in the presence of an antioxidant. In general, the DPPH radical is monitored at 517 nm (Fig. 1 (left)), at which the absorption decreases in the presence of antioxidants, and Fig. 1 (right) shows the percentage inhibition plotted against antioxidant concentration. From Table 1, it can be seen that all compounds, except for **4**, **6a**, **11**, **13**, **19**, and **21**, possess antioxidant properties. In particular, compound **3** showed the strongest antioxidant properties among all synthesized compounds with an IC_{50} of approximately 93.4 μM and comparable to those of vitamin C (IC_{50} ~ 141.9 μM). The IC_{50} values of the remaining compounds are decrease to approach the value of vitamin C in the order of **1** > **15** > **6c** > **6b** > **9** >**17** > **8**. Upon replacing the hydrogen with acetyl (*i.e.*, compound **4**) or with phenyl group (*i.e.*, compound **6a**) in the pyrazoline ring in compound **3**, no antioxidant activity is observed in both compounds. On the other hand, in the presence of an electron-donating or electron-withdrawing substituents like methyl and nitro in the para position for the phenyl group attached to the pyrazoline ring, the antioxidant activity of the pyrazoline compound **6c** and **6b** are increased compared with compound **6a**. Also, the antioxidant activity of

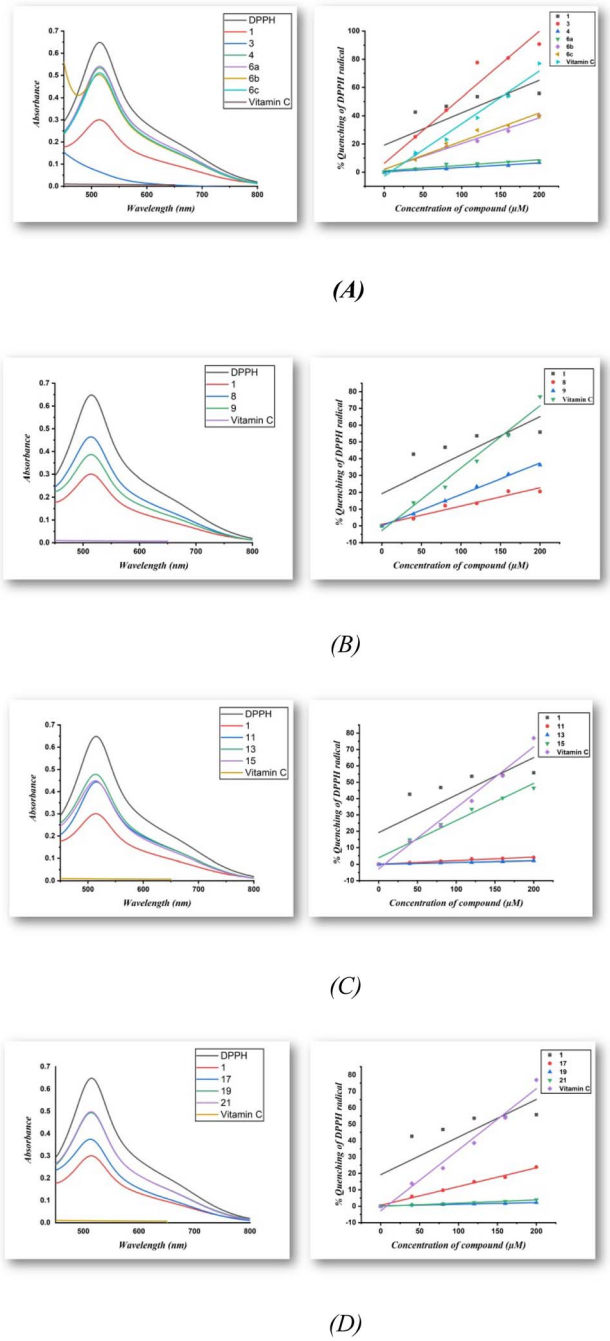

Fig. 1 (A–D) Typical absorption spectra of 100 μM of the DPPH radical alone and in presence of a 200 μM concentration of compounds and vitamin C (left) along with a diagram of the percentage of quenching of the DPPH radical against the concentration of the antioxidants compounds and vitamin C (right).

the oxime compound **8** (IC_{50}: 448.7 μM) is decreased compared with the isoxazoline **9** (IC_{50}: 267.9 μM). By comparing the amino pyrimidine **11** with the dimer product thiopyrimidine compound **15**, no antioxidant activity is observed for compound **11** while compound **15** exhibits good antioxidant properties. Furthermore, triazolo[1,5-*a*]pyrimidine compound **17** exhibits good antioxidant properties (IC_{50}: 432.90 μM) compared with

Table 1 IC_{50} values of afforded heterocyclic compounds (**1–21**) for the DPPH radical in methanol

Compounds	IC_{50} (μM)
1	134.26
3	93.40
4	—
6a	—
6b	263.01
6c	240.07
8	448.70
9	267.90
11	—
13	—
15	203.08
17	432.90
19	—
21	—
Vitamin C	141.90

imidazo[1,2-*a*]pyrimidine compound **19** which does not show any antioxidant activity. Accordingly, compounds **1** and **3** exhibit greater DPPH radical scavenging capacity than vitamin C as a reference compound, indicating that they are useful as antioxidants.

2.3. Docking analysis

The complex docking molecular analysis was enhanced with bond lengths in Å units using Moe software.[48] The minimization energies were then employed to maintain the geometrical optimization and systematic investigations with an RMS gradient of 0.01 Å. Also, the crystal structure of Klebsiella pneumoniae R204Q HpxO complexed with FAD (**PDBID:3RP8**),[49] as shown in Fig. 2 and Table 2. Chalcone **1** exhibited the highest binding affinity to the protein, with an energy affinity of −13.521 kcal mol^{-1} and the shortest distance ranging from 1.32–2.85 Å. This strong binding resulted from the hydrogen bond interactions between the OH group and the C=O group of chalcone, enabling a compact connection with the protein's amino group, specifically Glu 30 and Gly 9. Compound **3** also demonstrated strong compatibility with the protein 3RP8, having an energy affinity of −13.782 kcal mol^{-1} with its OH group, and binding to Asp254 at a distance of 1.31 Å. In contrast, compounds **4** and **6a** displayed reduced affinities, with energy levels of −12.624 and −10.625 kcal mol^{-1}, respectively, and increased interaction distances in the range of 2.52–2.62 Å. While compound **6a** did bind to Ser 350 through its OH group, compounds **6b** and **6c** showcased remarkable binding affinities with values of −12.524 and −12.841 kcal mol^{-1}, respectively. This was attributed to the presence of withdrawing (NO_2) and electron-donating (CH_3) groups that influenced their binding capabilities with proteins and enhanced hydrogen bond interactions. Furthermore, the reaction of chalcone with hydroxyl amine in different conditions showed different binding interactions in energy −10.025 kcal mol^{-1} and −11.254 kcal mol^{-1} for compounds **8** and **9**, respectively. Both compounds showed binding with OH of the phenyl ring with short bond lengths

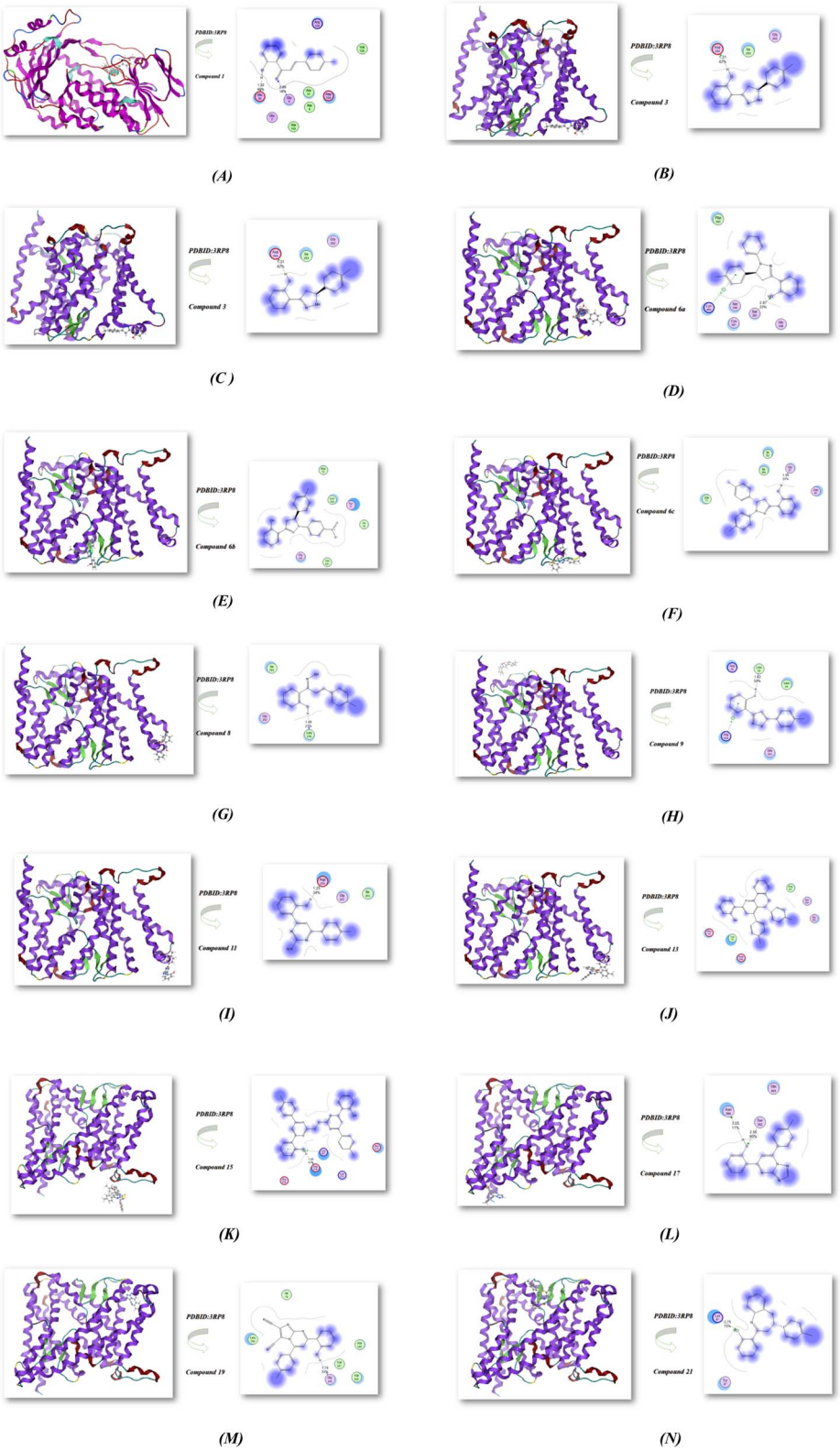

Fig. 2 (A–N) Molecular docking investigation of nitrogen heterocycles utilized PDBID:3RP8 protein.

1.48–1.43 Å with different amino acids (Leu 249, Gly 252, Ile 253) and (Leu 33, Leu 34, Arg 35, Arg 304, Gln 303); respectively. Moreover, the reactivity of chalcone with guanidine, urea and thiourea afford different heterocyclic compounds **11**, **13** and **15**. These compounds showed also least binding affinity with **PDBID:3RP8** with −10.521, −11.762 and −12.400 kcal mol^{-1}

Table 2 The molecular docking of synthesized compounds with PDBID:3RP8

(PDB:3RP8)

	Affinity of energy (kcal mol^{-1})	Distance (Å)	Amino acids		Affinity of energy (kcal mol^{-1})	Distance (Å)	Amino acids
1	−13.521	1.32, 2.85 Å	Glu 30, Gly 9, Gly 7, Ala8, Ala 31, Ala 153, Asp 154, Val 125	**9**	−11.254	1.43 Å	Leu 33, Leu 34, Arg 35, Arg 304, Gln 303
3	−13.782	1.31Å	Asp 254, Ile 253, Gly 252	**11**	−10.521	1.23 Å	Asp 254, Gly 252, Ile 253
4	−12.624	2.52 Å	Arg 125, Gly 189, Ser 302, Gly 187, Cys 188	**13**	−11.762	2.05 Å	Phe 251, Ser 250, Gly 252, Glu 75, Val 76, Asp 254
6a	−10.6257	2.67 Å	Ser 350, Cys 347,Gly 348, Ser 349, Lys 400	**15**	−12.400	1.28 Å	Lys 221, Asp 219, Glu 218, Lys 213, Glu 214
6b	−12.542	2.74 Å	Gly 342, Val 341, Leu 338, Tyr 77, ile 79	**17**	−9.6211	2.56,3.55 Å	Asn 299, Ser 302
6c	−12.841	1.54 Å	Gly 81, Asn 80, Ile 83, Ile 354	**19**	−8.0696	1.74 Å	Gly 342, Val 341, Val 345, Ala 346, Leu 338, Ile 79
8	−10.025	1.48 Å	Leu 249, Gly 252, Ile 253	**21**	−8.0052	2.75 Å	Lys 67, Tyr 87

and length ranges (1.23–2.05 Å). The interactions mainly occurred with the OH group of the phenyl ring but compound **15** showed compatibility with one OH group due it is a bis compound, leading to its increased stability when interacting with proteins such as (Lys 221, Asp 219, Glu 218, Lys 213, Glu 214). Also, the reactivity of chalcone with various nitrogen heterocyclic produced compounds **17**, **19**, and **21**. These compounds showed least binding affinities with values of −9.621, −8.0696, and −8.0052 kcal mol^{-1} and distance with range 1.74–3.55 Å. The binding mostly occurred with OH and amino group in amino acids with (Asn 299, Gly 342 and Lys 67; respectively). We concluded that the antioxidant activity was exhibited from hydrogen bonding interaction between OH group of the phenyl ring with DPPH radical scavenger which is be confirmed through docking investigation as displayed in Fig. 2(A–N).[50–53]

2.4. DFT study

2.4.1. Molecular orbital analysis and chemical reactivity. Full optimization was carried out for all produced compounds along with chalcone **1** using the DFT/B3LYP/6-31G(d,p) basis set,[54–56] as displayed in Fig. 3. A frequency calculation was done to guarantee that there were no imaginary frequencies. From eqn (1)–(8) estimated from B3LYP/6-31G(d,p), Table 3 lists the physical properties used in the optimization of molecular structures of all compounds concerning (σ) absolute softness, (χ) electronegativity, (ΔN_{max}) electronic charge, (η) absolute hardness, (ω) global electrophilicity, (S) global softness, and (Pi) chemical potential. Compared to the starting chalcone **1**, all synthesized compounds **3–21** showed higher energy stability, as well as thiopyrimidine **15**, which showed greater stability with energy (−2477.18 au) (−67407.34 e V) because of the presence of N, O, and S in its structure and increased electronegativity. Additionally, compound **19** has a very high dipole moment compared to other compounds. The difference in dipole moment between compound **19** and the chalcone **1** is 5.8 D, which is caused by the presence of two CN groups, which facilitates the separation of charges and increases reactivity.[3] A molecule's kinetic stability and chemical hardness-softness can be evaluated using the energy gap (ΔE) between its highest occupied molecular orbital (HOMO) and its lowest unoccupied molecular orbital (LUMO).[57–59] Consequently, the hardness and softness of the molecule are controlled by its ΔE, where large ΔE values indicate high kinetic stability, while low values indicate high chemical reactivity.[60] In addition, the hardness of a chemical system is a measure of its resistance to deformation of the electron cloud by small perturbations encountered during the chemical process. Therefore, the electron density of soft molecules can be easily altered unlike that of hard molecules. The ability of an electrophile to acquire electronic charge is described by electrophilicity, besides its resistance to exchanging electronic charge with its surroundings. Furthermore, it provides information about electron transfer (chemical potential) and stability (hardness), as well as a better understanding of global chemical reactivity.

Hard molecules have a huge HOMO–LUMO gap, whereas soft molecules have a small HOMO–LUMO gap. Furthermore, hard molecules tend to have high kinetic stability and low chemical reactivity, whereas soft molecules have the opposite properties. According to Table 3, the higher hardness values (2.27 eV) and low softness (0.43 eV) display lower intramolecular charge transfer present in compound **9**. Also, compound **9** has the highest ΔE among all compounds reflecting its kinetic stability, whereas compound **6b** has the lowest ΔE reflecting its high chemical reactivity. Fig. 4 illustrates the energy levels of HOMO–LUMO orbitals, while Fig. 5 shows their orbital analyses of LUMO and HOMO calculated at the B3LYP/6-31G(d, p) level for all compounds **1–21**. Positive and negative phases were characterized by red and green colors, respectively. For the start compound **1**, the electron clouds in the HOMO distribute over the π-electron of the two phenyl rings together with the double bond of the CH=CH group, the oxygen atom of the OH group, and the methyl group (*i.e.* the whole molecule except for the carbonyl group), while its LUMO distributes charges over the molecule except for the methyl group. For the produced heterocyclic compounds, the electron clouds in both HOMO and LUMO of compound **3** distribute charges over the entire

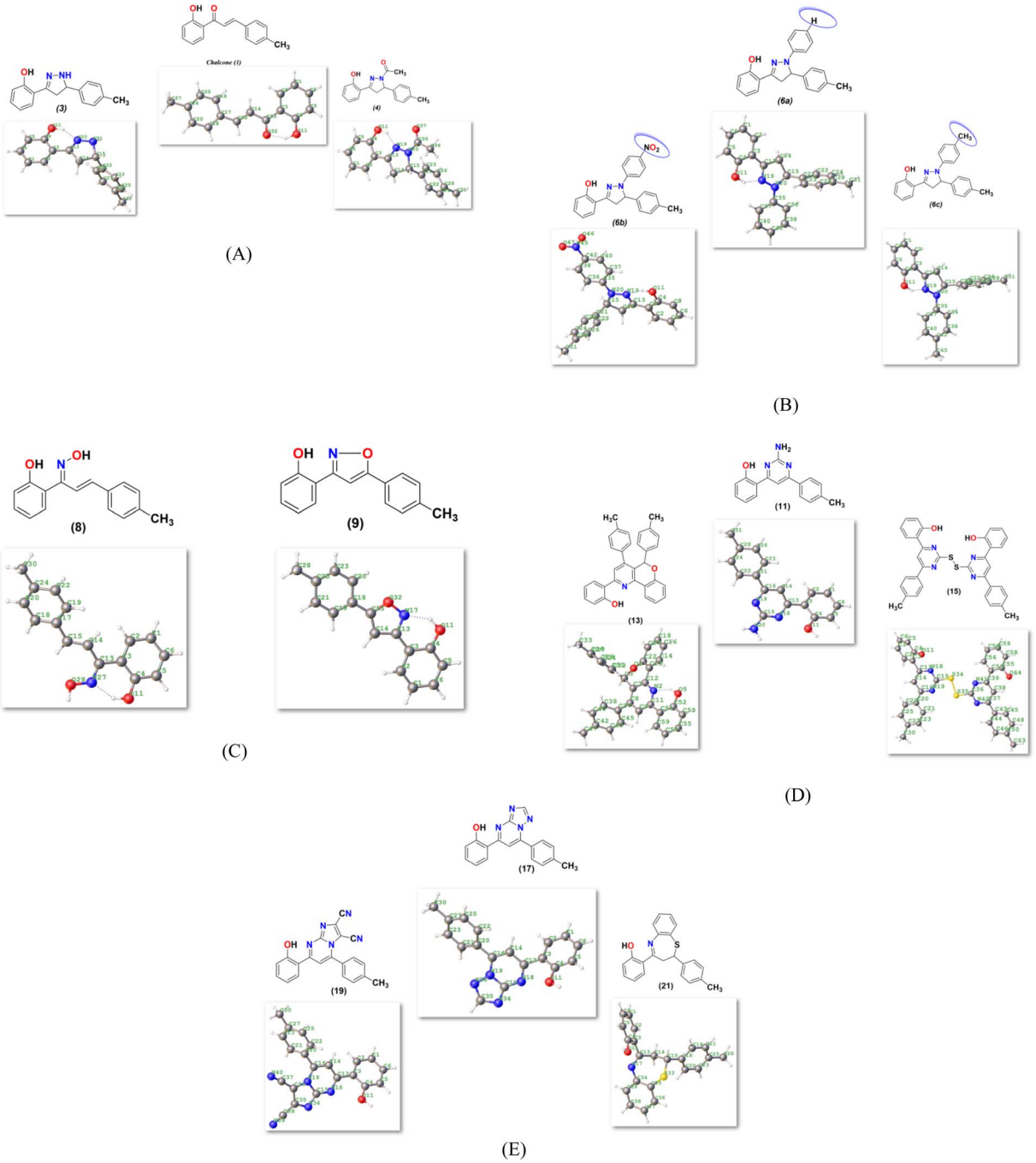

Fig. 3 (A–E) Chemical and the optimized structure of compounds **1–21** utilized DFT/631(G) basis set.

molecule except for the methyl group. Similar charge distribution was found in the HOMO of compound **4** except for the methyl group in both acetyl and tolyl group, while the electron clouds LUMO distribute charges over the entire molecule except for the tolyl group and the attached CH group in the pyrazolyl ring. The electronic clouds in compounds **6a**, **6b**, and **6c** behave similarly in a HOMO, where they are mainly distributed in the molecule except for the tolyl groups. Their LUMO differs based on the group that is attached to the second phenyl ring, where the H atom and the donating methyl group in compounds **6a** and **6c** distribute charges toward the hydroxyphenyl ring, whereas in compound **6b**, the electron withdrawing nitro group causes charges to be distributed towards the nitrophenyl ring, as shown in Fig. 5. Oxime **8** has different HOMO distribution charges than isoxazoline **9**, where the electron density is located on the entire molecule in compound **8**, whereas it is populated in the hydroxyphenyl ring and the isoxazoline ring in compound **9**. On the contrary, their LUMO electron clouds distribute the charges over the entire molecule of both compounds. The HOMO of the aminoprymidine **11** is localized

Table 3 Ground state energies of compounds utilizing DFT/B3LYP/6-31G(d,p) and their physical parameters

Physical descriptors												
Compound	E_T (au)	E_{HOMO} (eV)	E_{LUMO} (eV)	E_g (eV)	μ (D)	χ (eV)	η (eV)	σ (eV)	P_i (eV)	S (eV)	ω (eV)	ΔN_{max}
1	−768.61	−6.13	−2.35	3.77	4.78	4.24	1.88	0.52	−4.24	0.264	4.763	2.246
3	−804.07	−5.53	−1.11	4.42	4.01	3.33	2.21	0.45	−3.33	0.226	2.507	1.507
4	−956.74	−5.78	−1.43	4.35	6.63	3.61	2.17	0.46	−3.61	0.229	2.991	1.657
6a	−1035.13	−5.16	−1.28	3.88	3.91	3.22	1.94	0.51	−3.22	0.257	2.681	1.662
6b	−1239.64	−5.49	−2.31	3.18	9.10	3.90	1.59	0.62	−3.90	0.313	4.783	2.450
6c	−1074.45	−5.08	−1.26	3.82	3.76	3.17	1.91	0.52	−3.17	0.261	2.633	1.659
8	−823.90	−5.86	−1.85	4.01	3.40	3.86	2.00	0.49	−3.86	0.249	3.720	1.927
9	−822.72	−6.09	−1.53	4.56	4.76	3.81	2.27	0.43	−3.81	0.219	3.186	1.672
11	−896.37	−6.00	−1.51	4.49	1.71	3.76	2.24	0.44	−3.76	0.222	3.155	1.677
13	−1440.04	−5.80	−1.58	4.21	5.03	3.69	2.10	0.47	−3.69	0.237	3.233	1.751
15	−2477.18	−5.95	−1.90	4.05	2.06	3.93	2.02	0.49	−3.93	0.246	3.817	1.941
17	−988.59	−6.18	−2.01	4.17	5.07	4.10	2.08	0.48	−4.10	0.240	4.038	1.969
19	−1157.03	−6.25	−2.34	3.91	10.59	4.30	1.95	0.51	−4.30	0.256	4.730	2.199
21	−1377.96	−5.88	−1.45	4.43	2.52	3.66	2.21	0.45	−3.66	0.225	3.033	1.653

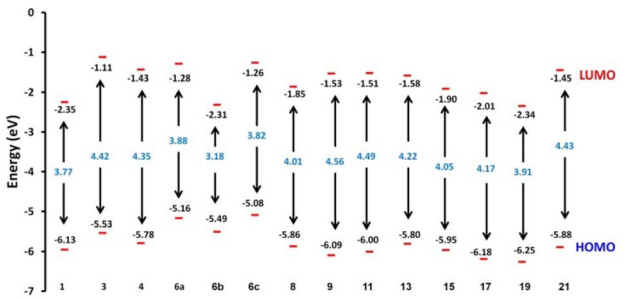

Fig. 4 Schematic diagrams of HOMO and LUMO energy levels of compounds **1–21** obtained from the DFT calculation with B3LYP/6-31G(d,p).

on the entire molecule, while the HOMO of the dimer of thiopyrimidine **15** is mainly localized on the center unit of disulfide bis-pyrimidine and part of charges distributed over one hydroxy phenyl ring and one benzene ring in the tolyl group. Their LUMO amost behave the same for both, where the LUMO of compound **11** is localized on the entire molecule except the amino group (*i.e.* pyrimidine, hydroxyphenyl, and tolyl group), while for compound **15** it is localized on the half unit of the dimer except sulfer (*i.e.* pyrimidine, hydroxyphenyl, and tolyl group). The HOMO for compound **13** is mostly localized on the 5*H*-chromeno[4,3-*b*]pyridine and phenol rings, while the LUMO is localized on the 5*H*-chromeno[4, 3-*b*]pyridine ring as reported.[46] The HOMO for both compounds **17** and **19** is localized on the whole molecule except the tolyl group, while their LUMO is localized on the whole molecule except the methyl group. The HOMO and LUMO for compound **21** are localized over the entire molecule except for the methyl group and little charge is distributed on the benzene ring of the tolyl group. Further, Mulliken atomic charges and electronic populations were determined using the B3LYP/6-31G(d, p) basis sets. Fig. S32 and S33† shows the atomic charges of all compounds **1–21**, and Fig. 3 shows their optimized structures with atomic numbers. Delocalization of negative charges in atoms with a lower electronegative results from electron attraction from atoms with a higher electronegative. Fig. S32 and S33† show that carbon atoms have both positive and negative charges. The heteroatoms (N and O) have negative charges and a high electron density. The carbon atoms that bonded to the S atom have negative charges. The most acidic hydrogens are the phenolic hydrogen in all compounds.[2,6]

$$\Delta E = E_{LUMO} - E_{HOMO} \quad (1)$$

$$\chi = \frac{-(E_{HOMO} + E_{LUMO})}{2} \quad (2)$$

$$\eta = \frac{(E_{LUMO} - E_{HOMO})}{2} \quad (3)$$

$$\sigma = 1/\eta \quad (4)$$

$$\mathrm{Pi} = -\chi \quad (5)$$

$$S = 1/2\eta \quad (6)$$

$$\omega = \mathrm{Pi}^2/2\eta \quad (7)$$

$$\Delta N_{max} = -\mathrm{Pi}/\eta \quad (8)$$

2.4.2. Molecular electrostatic potential (MEP). MEP mapping, a tool for analyzing and predicting molecular behavior, was used to identify electrophilic and nucleophilic active sites and hydrogen bonding interactions.[46,61] This tool allows visualization of the charge distribution and helps comprehend the relative polarity of a molecule and predict their reactive sites. Also, this method is extremely helpful for determining relationships between physicochemical properties and molecular structure. In MEP mapping, red represents electron-rich, nucleophilic regions, while blue represents electron-poor, electrophilic regions. Different colors describe the electrostatic

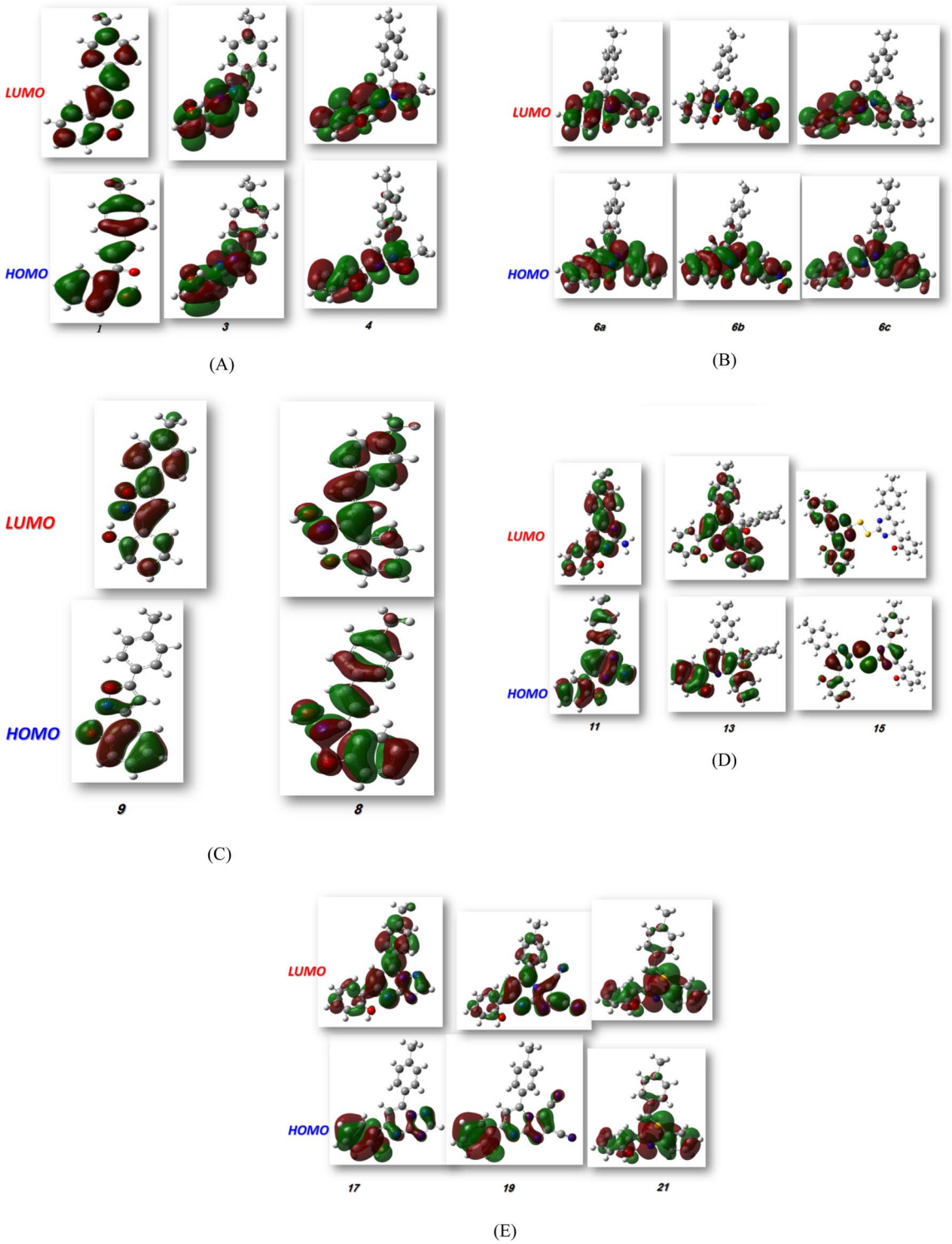

Fig. 5 (A–E) FMO profiles of synthesized heterocyclic compounds.

potential on the surface, decreasing from blue to green to yellow to orange to red. Based on full-geometry optimization at DFT/B3LYP/6-31G (d,p) level, MEP was calculated for the two most active antioxidant compounds (compound **1** and compound **3**). A detailed analysis of the MEP maps (Fig. 6) indicates that the highly negative electrostatic potential regions (red) are centered on the oxygen atoms of the OH group and the ketone group in compound 1 with values of -5.124×10^{-2} eV (at an isovalue of 0.001 electrons per Å^3), while the highly positive regions (blue color) are concentrated near the olefin proton. For compound **3**, the negative values are mainly located over the oxygen atom of the hydroxyl group with a value of -5.316×10^{-2} eV, indicating

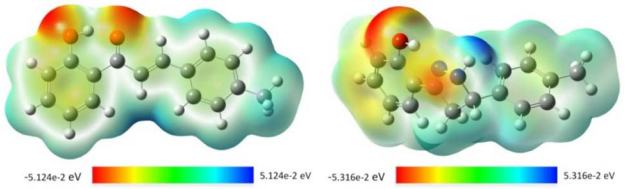

Fig. 6 Molecular electrostatic potential (MEP) maps of chalcone **1** (left) and compound **3** (right).

a potential electrophilic attack site, while the most positive regions were localized on the H19 of the NH group with a value of -5.316×10^{-2} eV, indicating a potential nucleophile attack site. Based on these findings, we are able to predict the probable sites for electrophilic attacks, which would clarify the docking results in regard to the binding of each molecule to the amino acid residues of the studied protein's active site.[62,63]

3. Experimental section

3.1. General procedure

The Gallenkamp melting point instrument was used to measure the melting points. Thin-layer chromatography (TLC) was conducted on Polygram SIL G/UV254 TLC plates, and the results were visualized with ultraviolet light at 254 nm and 350 nm. In this study, the CEM Discover LabMate microwave apparatus (300 W, ChemDriver software; Matthews, NC) was used for microwave experiments. In closed vessels under pressure, microwave irradiated Pyrex tubes with PCS caps were used to conduct the reactions. A Bruker DPX 400 superconducting NMR spectrometer was used to record the ^{1}H and ^{13}C nuclear magnetic resonance (NMR) spectra, and the IR spectra were measured with a Jasco Fourier transform/IR-6300 FT-IR spectrometer. The Elementar Vario MICRO Cube was used for the elemental analysis. Electron impact (EI) was used to determine mass analyses on a Thermo double-focusing sector (DFS) mass spectrometer. Varian Cary 5 spectrometer and a Shimadzu UV2600 spectrophotometer were used in UV-vis studies. Utilizing X-ray microdiffraction and single-crystal X-ray diffractometers, Rigaku D/MAX Rapid II and Bruker X8 Prospector were used to determine the X-ray crystal structure.

3.2. Materials and reagents

1-(2-Hydroxyphenyl)ethan-1-one, 4-methylbenzaldehyde were purchased from Aldrich Chemical CO that was used in the synthesis of chalcone **1** as reported in the literature.[46,64] In this study, all solvents were obtained from Aldrich.

3.2.1. Synthesis of 2-(5-(*p*-tolyl)-4,5-dihydro-1H-pyrazol-3-yl)phenol (3).[42] A mixture of chalcone **1**[46] (1 g, 4.2 mmol) and hydrazine hydrate (10 equivalent) in ethanol (8 mL) was mixture was irradiated utilizing microwave at 70 °C for 30 min. White crystals was formed after cooling and filtered. Yield (0.8 g, 76%), M p 106 °C (literature:[65] 105–106 °C). FT-IR (ν_{max}, cm^{-1}): 3339 (NH), 3006 (C–H Ar), 1619 (C=N). ^{1}H NMR (DMSO-d_6, δ ppm): 2.28 (s, 3H, H_3C), 2.94–2.98 (dd, 1H, J = 10.8 Hz, H-4$_A$), 3.56–3.60 (dd, 1H, J = 10.8 Hz, H-4$_B$), 4.79–4.83 (dt, 1H, J = 10.8 Hz, H-5$_X$), 6.86–6.91 (m, 2H, ArH), 7.15 (d, 2H, J = 7.8 Hz, ArH), 7.21–7.29 (m, 4H, ArH), 7.80 (d,1H, HN), 11.16 (s, 1H, HO), ^{13}C NMR (DMSO-d_6):δ 20.6 (CH_3), 40.78 (CH), 61.84 (CH), 115.69 (C), 116.76 (CH), 119.10 (CH), 126.59 (CH), 127.72 (CH), 128.98 (CH), 129.67 (C), 136.43 (C), 139.22 (C), 152.46 (C), 156.71 (C). MS (m/z): 252 (M^+, 100.0%), anal. calcd. for $C_{16}H_{16}N_2O$ (252.13): C, 76.16; H, 6.39; N, 11.10. Found: C, 76.00; H, 6.41; N, 11.08.

3.2.2. Synthesis of 1-(3-(2-hydroxyphenyl)-5-(*p*-tolyl)-4,5-dihydro-1H-pyrazol-1-yl)ethan-1-one (4). A mixture of **1** (1 g, 4.2 mmol) and hydrazine hydrate (10 equivalent) in glacial acetic acid (5 mL) was irradiated utilizing microwave at 70 °C for 30 min. The reaction mixture was cooled and poured onto crushed ice. The obtained precipitate was filtered, washed with H_2O, dried, and recrystallized from ethanol to afford **7**. Yield (1.08 g, 87.8%). Mp 131 °C (literature:[65] 131–134 °C). FT-IR (ν_{max}, cm^{-1}): 3032 (C–H Ar), 1648 (C=O), 1615 (C=N). ^{1}H NMR (DMSO-d_6, δ ppm): 2.26 (s, 6H, 2 H_3C), 3.21 (dd, 1H, J = 18.6 Hz, H-4$_A$), 3.90 (dd, 1H, J = 18.6 Hz, H–4$_B$), 5.44 (dd, 1H, J = 12 Hz, H-5$_X$), 6.90 (t, 1H, J = 8.4 Hz, ArH), 6.96 (d, 1H, J = 7.2 Hz, ArH), 7.08–7.18 (m, 4H, ArH), 7.33 (t,1H, J = 8.4 Hz, ArH), 7.55 (d,1H, J = 7.8 Hz, ArH), 10.20 (s, 1H, HO), ^{13}C NMR (DMSO-d_6):δ 20.6 (CH_3), 21.7 (CH_3), 43.58 (CH_2), 58.16 (CH), 116.23 (C), 119.54 (CH), 125.39 (CH), 129.01 (CH), 131.79 (CH), 136.36 (C), 139.26 (C), 155.65 (C), 156.69 (C), 166.88 (*C*O). MS (m/z): 294 (M^+, 100.0%), anal. calcd. for $C_{18}H_{18}N_2O_2$ (294.14): C, 73.45; H, 6.16; N, 9.52. Found: C, 73.40; H, 6.20; N, 9.49.

3.2.3. Synthesis of 2-(1-phenyl-5-(*p*-tolyl)-4,5-dihydro-1H-pyrazol-3-yl)phenol (6a). A mixture of chalcone **1** (1 g, 4.2 mmol), phenylhydrazine (0.45 g, 4.2 mmol) in dry EtOH (8 mL) was irradiated utilizing microwave at 70 °C for 30 min. The reaction mixture poured into ice water. Yield (0.3 g, 21.8%). M p 133–134 °C. FT-IR (ν_{max}, cm^{-1}): 3155 (OH), 3093 (C–H Ar), 1616 (C=N). ^{1}H NMR (DMSO-d_6, δ ppm): 2.25 (s, 3H, H_3C), 3.21 (dd, 1H, J = 17.4 Hz, H-4$_A$), 4.01 (dd, 1H, J = 17.4 Hz, H-4$_B$), 5.40 (dd, 1H, J = 12 Hz, 5$_X$), 6.75 (t, 1H, J = 7.2 Hz, ArH), 6.91–6.93 (m, 3H, ArH), 6.97–6.99 (dd, 1H, J = 8.4 Hz, ArH), 7.14 (d, 2H, J = 7.8 Hz, ArH), 7.17–7.21 (m, 4H, ArH), 7.26–7.29 (m, 1H, ArH), 7.40 (d, 1H, J = 18.6 Hz, ArH),10.55 (s, 1H, HO), ^{13}C NMR (DMSO-d$_6$): δ 20.62 (CH_3), 43.84 (CH_2), 61.97 (CH), 112.92 (C), 116.04 (CH), 116.58 (CH), 119.14 (CH), 125.88 (CH), 128.04 (CH), 129.05 (CH), 129.65 (CH), 130.37 (CH), 136.71 (C), 139.10 (C), 143.65 (C), 149.98 (C), 156.19 (C). MS (m/z): 328 (M^+, 100.0%), anal. calcd. for $C_{22}H_{20}N_2O$ (328.16): C, 80.46; H, 6.14; N, 8.53. Found: C, 80.39; H, 6.20; N, 8.48.

3.2.4. Synthesis of 2-(1-(4-nitrophenyl)-5-(*p*-tolyl)-4,5-dihydro-1H-pyrazol-3-yl)phenol (6b). A mixture of chalcone **1** (1 g, 4.2 mmol), 4-nitrophenylhydrazine hydrochloride (0.79 g, 4.2 mmol) in dry EtOH (8 mL) was irradiated utilizing microwave at 70 °C for 30 min. The red precipitate which formed was filtered. Yield (1.36 g, 87%). M p 208–210 °C. FT-IR (ν_{max}, cm^{-1}): 3329 (OH), 3093 (C–H Ar), 1620 (C=N). ^{1}H NMR (DMSO-d_6, δ ppm): 2.24 (s, 3H, H_3C), 3.33–3.39 (m, 1H, H-4$_A$), 4.08 (dd, 1H, J = 18 Hz, H-4$_B$), 5.65 (dd, 1H, J = 11.4 Hz, H-5$_X$), 6.94–7.06 (m, 4H, ArH), 7.15 (1, 4H, J = 19.8 Hz, ArH), 7.32 (dt, 1H, J = 3.6 Hz, ArH), 7.62 (dd, J = 7.8 Hz, 1H, ArH), 8.06 (d, 2H, J = 9.6 Hz, ArH), 10.22 (s, 1H, HO), ^{13}C NMR (DMSO-d_6): δ 20.61 (CH_3), 44.87

(CH_2), 61.10 (CH), 111.86 (C), 116.49 (CH), 119.62 (CH), 125.57 (CH), 125.81 (CH), 128.76 (CH), 128.97 (CH), 129.76 (CH), 131.50 (C), 137.06 (C), 137.99 (C), 147.67 (C), 154.00 (C), 156.32 (C). MS (*m*/*z*): 373 (M^+, 55.0%), anal. calcd. for $C_{22}H_{19}N_3O_3$ (373.14): C, 70.76; H, 5.13; N, 11.25. Found: C, 70.69; H, 5.20; N, 11.20.

3.2.5. Synthesis of 2-(1,5-di-*p*-tolyl-4,5-dihydro-1H-pyrazol-3-yl)phenol (6c). A mixture of chalcone **1** (1 g, 4.2 mmol), *p*-tolylhydrazine hydrochloride (0.66 g, 4.2 mmol) in dry EtOH (8 mL) was irradiated utilizing microwave at 70 °C for 30 min. The reaction mixture poured into ice water and the beige precipitate which formed was filtered. Yield (0.2 g, 13.9%). M p 144–145 °C. FT-IR (ν_{max}, cm^{-1}): 3555 (OH), 3095 (C–H Ar), 1615 (C=N). ^{1}H NMR (DMSO-d_6, δ ppm): 2.16 (s, 3H, H_3C), 2.25 (s, 3H, H_3C), 3.19 (dd, 1H, J = 18 Hz, H-4_A), 3.98 (dd, 1H, J = 16.8 Hz, H-4_B), 5.35 (dd, 1H, J = 12 Hz, H-5_X), 6.81 (d, 2H, J = 8.4 Hz, *H*–ArH), 6.89 (t, 1H, J = 7.8 Hz, ArH), 6.96–7.00 (m, 3H, ArH), 7.13 (d, 2H, J = 7.8 Hz, ArH), 7.18 (d, J = 8.4 Hz, 2H, ArH), 7.25–7.28 (dt, J = 8.4 Hz, 1H, ArH), 7.38 (dd, 1H, J = 7.8 Hz, ArH), 10.58 (s, 1H, HO), ^{13}C NMR (DMSO-d_6):δ 20.05 (CH_3), 20.61 (CH_3), 43.70 (CH_2), 62.32 (CH), 113.16 (C), 115.98 (CH), 116.61 (CH), 119.50 (CH), 125.95 (CH), 127.91 (CH), 129.46 (CH), 130.20 (C), 136.65 (C), 139.09 (C), 141.60 (C), 149.57 (C), 156.15 (C). MS (*m*/*z*): 342 (M^+, 100.0%), anal. calcd. for $C_{22}H_{19}N_3O_3$ (342.17): C, 80.67; H, 6.48; N, 8.18. Found: C, 80.63; H, 6.40; N, 8.20.

3.2.6. Synthesis of 1-(2-hydroxyphenyl)-3-(*p*-tolyl)prop-2-en-1-one oxime (8). A mixture of chalcone **1** (1 g, 4.2 mmol), hydroxylamine hydrochloride (0.43 g, 4.2 mmol) and NaOAc (0.68 g, 8.4 mmol) in ethanol (5 mL) was irradiated at 70 °C for 30 min using microwave. The reaction mixture was poured into ice water to give a white precipitate (0.3 g, 23.5%). M p 174–176 °C (literature:[66] 174–176 °C). FT-IR (ν_{max}, cm^{-1}): 3321 (OH), 3028 (C–H Ar), 1635 (C=N). ^{1}H NMR (DMSO-d_6, δ ppm): 2.29 (s, 3H, H_3C), 6.42 (d, 1H, J = 16.8 Hz, CH=CH), 6.85 (dt, 1H, J = 7.8 Hz, ArH), 6.89 (dd, 1H, J = 7.8 Hz, ArH), 7.14 (m, 2H, ArH), 7.23 (t, 2H, J = 8.4 Hz, ArH), 7.37 (d, 2H, J = 8.4 Hz, ArH), 7.50 (d, 1H, J = 16.8 Hz, CH=CH), 9.65 (s, 1H, N–HO), 11.35 (s, 1H, HO), ^{13}C NMR (DMSO-d_6): δ 20.72 (CH_3), 115.83 (CH), 116.26 (C), 118.74 (CH), 121.92 (CH), 127.03 (CH), 129.42 (CH), 129.76 (CH), 130.83 (CH), 133.37 (CH), 135.94 (C), 138.37 (C), 154.56 (C), 155.69 (C). MS (*m*/*z*): 253 (M^+, 60.0%), anal. calcd. for $C_{16}H_{15}NO_2$ (253.11): C, 75.87; H, 5.97; N, 5.53. Found: C, 75.82; H, 5.93; N, 5.50.

3.2.7. Synthesis of 2-(5-(p-tolyl)isoxazol-3-yl)phenol (9).[67] A mixture of chalcone **1** (1 g, 4.2 mmol), hydroxylamine hydrochloride (0.43 g, 4.2 mmol) and NaOH (0.25 g, 6.25 mmol) in ethanol (8 mL) was irradiated at 70 °C for 30 min using microwave. The reaction mixture was poured into ice water to give a beige precipitate (0.1 g, 9.5%). M p 142–143 °C (literature:[66] 142–143 °C). FT-IR (ν_{max}, cm^{-1}): 3281 (OH), 3028 (C–H Ar), 1607 (C=N). ^{1}H NMR (DMSO-d_6, δ ppm): 2.32 (s, 3H, H_3C), 7.38 (d, 1H, J = 12 Hz, ArH), 7.45 (t, 1H, J = 12 Hz, ArH), 7.75–7.83 (m, 3H, ArH), 8.11 (m, 4H, ArH), 9.53 (s, 1H, HO), ^{13}C NMR (DMSO-d_6): δ 21.02 (CH_3), 118.36 (CH), 121.29 (C), 124.50 (CH), 124.75 (CH), 127.56 (CH), 128.49 (C), 129.12 (CH), 133.62 (CH), 138.73 (CH), 139.78 (C), 145.4 (C), 154.50 (C), 172.84 (C). MS (*m*/*z*): 252 ($(M + H)^+$, 100.0%), anal. calcd. for $C_{16}H_{13}NO_2$ (251.09): C, 76.48; H, 5.21; N, 5.57. Found: C, 76.52; H, 5.29; N, 5.50.

3.2.8. Synthesis of 2-(2-amino-6-(*p*-tolyl)pyrimidin-4-yl) phenol (11). A mixture of compound **1** (1.0 g, 4.2 mmol), guanidine (0.4 g, 4.2 mmol) and KOH (0.47 g, 8.4 mmol) was dissolved in EtOH (8 mL) and irradiated at 70 °C for 1.5 h using microwave. After the accomplishment of reaction (as examined through TLC), the entire mixture was poured on to crushed ice to give a yellow precipitate which was filtered, washed successively with water and dried. Yield (0.1 g, 8.6%). M p 214 °C (literature:[68] 191–192 °C). FT-IR (ν_{max}, cm^{-1}): 3356 (OH), 3259 (NH), 3089 (C–H Ar), 1672 (C=N). ^{1}H NMR (DMSO-d_6, δ ppm): 2.39 (s, 3H, H_3C), 6.90 (m, 2H, H-3′, 5′), 7.17 (s, 2H, H_2N), 7.33–7.37 (m, 3H, ArH), 7.79 (s, 1H, ArH), 8.15 (d, 2H, J = 12.6 Hz, ArH), 8.21 (d, 1H, J = 12.6 Hz, ArH), 14.03 (s, 1H, HO), ^{13}C NMR (DMSO-d_6): δ 20.97 (CH_3), 99.49 (CH), 117.55 (CH), 118.05 (CH), 118.62 (C), 127.10 (CH), 128.01 (CH), 129.24 (CH), 132.58 (CH), 134.20 (C), 140.68 (C), 160.34 (C), 165.07 (C), 165.23 (C). MS (*m*/*z*): 277 (M^+, 100.0%), anal. calcd. for $C_{17}H_{15}N_3O$ (277.12): C, 73.63; H, 5.45; N, 15.15. Found: C, 73.67; H, 5.52; N, 15.10.

3.2.9. Synthesis of 2-(4,5-di-*p*-tolyl-5H-chromeno[4,3-*b*] pyridin-2-yl)phenol (13).[46] A mixture of compound **1** (1.0 g, 4.2 mmol), urea (0.25 g, 4.2 mmol) and KOH (0.47 g, 8.4 mmol) was dissolved in EtOH (8 mL) and irradiated at 70 °C for 1.5 h using microwave. After the accomplishment of reaction (as examined through TLC), the entire mixture was poured on to crushed ice to give a yellow precipitate which was filtered, washed successively with water and dried. Yield (0.1 g, 5.2%). M p 86 °C. FT-IR (ν_{max}, cm^{-1}): 3053 (C–H Ar), 1600 (C=N). ^{1}H NMR (DMSO-d_6, δ ppm): 2.20 (s, 3H, H_3C), 2.35 (s, 3H, H_3C), 6.44 (s, 1H, H-5), 6.93–7.07 (m, 7H, ArH), 7.15 (t, 1H, J = 10.8 Hz, ArH), 7.22–7.27 (m, 4H, ArH), 7.33–7.40 (m, 2H, ArH), 7.99 (d, 1H, J = 10.2 Hz, ArH), 8.10 (s, 1H, ArH), 8.18 (d, 1H, J = 10.8 Hz, ArH), 13.80 (s, 1H, HO), ^{13}C NMR (DMSO-d_6): δ 20.59 (CH_3), 20.73 (CH_3), 99.49 (CH), 117.72 (C), 118.17 (CH), 119.17 (CH), 119.27 (CH), 120.56 (C), 121.85 (C), 122.50 (CH), 122.85 (CH), 123.55 (CH), 127.65 (CH), 127.95 (CH), 128.27 (CH), 129.12 (CH), 129.23 (CH), 131.65 (CH), 132.28 (CH), 133.58 (C), 135.60 (C),137.99 (C), 138.41 (C), 145.33 (C), 149.40 (C), 153.71 (C), 156.36 (C), 158.76 (C). MS (*m*/*z*): 455 (M^+, 70.0%), anal. calcd. for $C_{32}H_{25}NO_2$ (455.19): C, 84.37; H, 5.53; N, 3.07. Found: C, 84.36; H, 5.53; N, 3.05.

3.2.10. Synthesis of 2,2'-(disulfanediylbis(6-(*p*-tolyl) pyrimidine-2,4-diyl))diphenol (15). A mixture of compound **1** (1.0 g, 4.2 mmol), thiourea (0.319 g, 4.2 mmol) and KOH (0.47 g, 8.4 mmol) was dissolved in EtOH (8 mL) and irradiated at 70 °C for 1.5 h using microwave. After the accomplishment of reaction (as examined through TLC), the entire mixture was poured on to crushed ice to give a yellow precipitate which was filtered, washed successively with water and dried. Yield (0.17 g, 7%). M p 248–250 °C. FT-IR (ν_{max}, cm^{-1}): 3019 (C–H Ar), 1613 (C=N). ^{1}H NMR (DMSO-d_6, δ ppm): 2.39 (s, 3H, H_3C), 6.88–6.93 (m, 4H, ArH), 7.34 (d, 6H, J = 12 Hz, ArH), 8.19 (d, 6H, J = 16.2 Hz, ArH), 8.52 (s, 2H, ArH), ^{13}C NMR (DMSO-d_6): δ 21.05 (CH_3), 109.70 (CH), 117.95 (CH), 119.42 (CH), 127.50 (C), 129.04 (CH′), 129.72 (CH), 132.46 (CH), 133.61 (CH), 142.17 (C), 159.10 (C), 164.71 (C), 165.05, (C), 165.31 (C), 166.63 (C). MS (*m*/*z*): 585 ($(M - H)^+$,

97.0%), anal. calcd. for $C_{34}H_{26}N_4O_2S_2$ (586.15): C, 69.60; H, 4.47; N, 9.55. Found: C, 69.56; H, 4.50; N, 9.49.

3.2.11. Synthesis of 2-(7-(*p*-tolyl)-[1,2,4]triazolo[1,5-*a*] pyrimidin-5-yl)phenol (17). A solution of chalcone **1** (1 g, 4.2 mmol) and 3-amino-1,2,4-triazole (0.35 g, 4.2 mmol) in DMF (5 mL) was irradiated at 70 °C for 30 min using microwave. The reaction mixture was cooled to room temperature, diluted with water (50 mL) and stirred sufficiently. The resulting mixture was filtered and washed with water to give the crude product, which was further purified by recrystallization from ethanol. Yellow precipitate, yield (0.71 g, 56.3%). Mp > 300 °C. FT-IR (ν_{max}, cm^{-1}): 3336 (OH), 3089 (C–H Ar), 1687 (C=N). ^{1}H NMR (DMSO-d_6, δ ppm): 2.46 (s, 3H, H_3C), 7.02–7.07 (m, 2H, ArH), 7.45–7.49 (m, 3H, ArH), 8.18 (d, 2H, J = 12.6 Hz, ArH), 8.22 (s, 1H, ArH), 8.28 (d, 1H, J = 12 Hz, ArH), 8.72 (s, 1H, ArH), 12.38 (s, 1H, *H*O), ^{13}C NMR (DMSO-d_6): δ 21.12 (CH_3), 107.07 (CH), 117.80 (CH), 119.44 (CH), 119.55 (C), 126.90 (CH), 129.20 (CH), 129.73 (CH), 129.84 (C), 133.34 (CH), 142.05 (C), 147.66 (C), 154.21 (C-3a), 155.76 (CH), 158.79 (C), 161.28 (C). MS (m/z): 302 (M^+, 100.0%), anal. calcd. for $C_{18}H_{14}N_4O$ (302.12): C, 71.51; H, 4.67; N, 18.53. Found: C, 71.48; H, 4.65; N, 18.50.

3.2.12. Synthesis of 7-(2-hydroxyphenyl)-5-(*p*-tolyl)imidazo [1,2-*a*]pyrimidine-2,3-dicarbonitrile (19). A solution of chalcone **1** (1 g, 4.2 mmol) and 2-amino-1*H*-imidazole-4,5-dicarbonitrile (0.55 g, 4.2 mmol) in DMF (5 mL) was irradiated at 70 °C for 30 min using microwave. The reaction mixture was cooled to room temperature, filtered and washed with water to give the crude product. Yellow precipitate, yield (0.16 g, 11%). Mp 247–250 °C. FT-IR (ν_{max}, cm^{-1}): 3189 (C–H Ar), 2246, 2228 (CN), 1614 (C=N). ^{1}H NMR (DMSO-d_6, δ ppm): 2.32 (s, 3H, H_3C), 7.02 (t, 1H, J = 7.2 Hz, ArH), 7.06 (d, 1H, J = 9 Hz, ArH), 7.45–7.49 (m, 3H, ArH), 7.67 (d, 2H, J = 8.4 Hz, ArH), 8.14 (s, 1H, ArH), 8.18 (d, 1H, J = 7.8 Hz, ArH), 11.68 (s, 1H, HO), ^{13}C NMR (DMSO-d_6): δ 21.14 (CH_3), 102.64 (C-3), 108.23 (CH), 112.43 (CN), 112.55 (CN), 117.7 (CH), 119.78 (CH), 126.91 (C), 127.24 (CH), 129.04 (CH), 129.22 (CH), 129.42 (C), 130.19 (C), 134.00 (CH), 141.87 (C), 148.38 (C), 149.03 (C-8a), 158.50 (C), 162.07 (C). MS (m/z): 351 (M^+, 100.0%), anal. calcd. for $C_{21}H_{13}N_5O$ (351.11): C, 71.79; H, 3.73; N, 19.93. Found: C, 71.71; H, 3.77; N, 19.89.

3.2.13. Synthesis of 2-(2-(p-tolyl)-2,3-dihydrobenzo[b][1,4] thiazepin-4-yl)phenol (21).[47] To a flask containing an equimolar mixture (4.2 mmol) of chalcone **1** (1 g) and 2-aminothiophenol (0.5 g) in methanol (8 mL), drops of piperidine was added, and the mixture was irradiated at 70 °C for 10 min using microwave. Filter the formed yellow precipitate. Yield (1.28, 88.8%). Mp 152–154 °C (literature:[47] 156–158 °C). FT-IR (ν_{max}, cm^{-1}): 3428 (OH), 3051 (C–H Ar), 1598 (C=N). ^{1}H NMR (DMSO-d_6, δ ppm): 2.28 (s, 3H, H_3C), 2.90 (t, 1H, J = 13.2 Hz, H-1_A), 3.50 (dd, 1H, J = 13.2 Hz, H–1_B), 5.22 (dd, 1H, J = 12.6 Hz, H-2_X), 6.95 (t, 1H, J = 8.4 Hz, ArH), 6.99 (d, 1H, J = 7.8 Hz, ArH), 7.12 (d, 2H, J = 7.8 Hz, ArH), 7.23 (d, 2H, J = 8.4 Hz, ArH), 7.27 (dt, 1H, J = 7.8 Hz, ArH), 7.37 (dd, 1H, J = 7.8 Hz, ArH), 7.45 (dt, 1H, J = 7.2 Hz, ArH), 7.56–7.60 (m, 2H, ArH), 7.86 (d, 1H, J = 7.8 Hz, ArH), ^{13}C NMR (DMSO-d_6): δ 20.65 (CH_3), 36.44 (CH_2), 58.86 (CH), 117.67 (CH), 118.06 (CH), 118.86 (C), 123.55 (CH), 125.35 (CH), 125.92 (CH), 126.61 (C-9a), 129.05 (CH), 129.79 (CH), 130.29 (CH), 133.79 (CH), 136.02 (CH), 136.94 (C), 140.84 (C), 148.35 (C-5a), 161.68 (C), 174.11 (C). MS (m/z): 345 (M^+, 20.0%), anal. calcd. for $C_{22}H_{19}NOS$ (345.12): C, 76.49; H, 5.54; N, 4.05. Found: C, 76.41; H, 5.49; N, 3.93.

3.3. Antioxidant activities

DPPH (2,2-diphenyl-1-picrylhydrazyl) radical scavenging activity. The scavenging activity of different heterocyclic compounds were determined using the free radical DPPH (2,2-diphenyl-1-picrylhydrazyl). Equal volumes of 100 μM DPPH chemical solution was mixed in methanol and added to different concentrations of the test compounds (0–200 μM mL^{-1}) in methanol and mixed well. The reaction mixture was incubated for 30 min at room temperature in the dark and was then measured at 520 nm. Plotting the percentage $DPPH^{\cdot}$ scavenging against concentration gave the standard curve and the percentage scavenging was calculated from the following equation:

$$\% \text{ scavenging} = [(\text{Absorbance of blank} - \text{Absorbance of test})/\text{Absorbance of blank}] \times 100$$

IC_{50} was obtained from a plot between concentration of test compounds and % scavenging. Ascorbic acid (vitamine C) was used as standard for comparison.

3.4. Molecular docking simulation

The complex docking molecular analysis was enhanced with bond lengths in Å units using Moe software.[48,69] Afterwards, with an RMS gradient of 0.01, the minimization energies were put into practise to sustain the geometrical optimisation and systematic studies, also Crystal Structure of Klebsiella pneumoniae R204Q HpxO complexed with FAD (**PDBID:3RP8**)[49] The authorization described by E-conformation, overall statistics, and connected to amino acids around the protein's binding compact.[70]

3.5. Computational studies

Molecular geometry was directly taken from the experimental outcomes of X-ray diffraction without any constraints. Density functional theory including Becke's three-parameter hybrid functional using the LYP correlation functional (B3LYP) with the 6-31G(d, p) basis set *via* the Berny method[54,55] were proceeded with the Gaussian 09W program[71] In order to investigate the reactive sites for compound **1** and **3**, the molecular electrostatic potential was calculated using the B3LYP/6-31G(d, p) method. Furthermore, the Mulliken atomic charges of all heterocyclic compounds were calculated as well.

4. Conclusions

In the present work, the reaction of chalcone with different nitrogen-containing investigated to form N-, S-, and O-containing heterocycles. The resulting heterocyclic compounds were confirmed by spectroscopic analyses, including FTIR, UV-visible, NMR, and mass spectrometry. The

antioxidant activity of these compounds was studied for their efficacy as antioxidants through their ability to scavenge the synthetic radicals 2,2-diphenyl-1-picrylhydrazyl (DPPH). Compound **3** (IC_{50} = 93.4 μM) and compound **1** (IC_{50} = 134.26 μM) showed the highest antioxidant activity, indicating their potential as antioxidants. On the other hand, compound **8** (IC_{50} = 448.70 μM) exhibited the lowest activity when compared to vitamin C (IC_{50} ~ 141.9 μM). In addition, the docking estimations were compatible with experimental results for these heterocyclic compounds evaluated with **PDBID:3RP8**. Furthermore, DFT/B3LYP/6-31G(d,p) basis sets were used to optimize the compounds and identify their Global reactivity descriptors, including HOMO–LUMO gaps, electronic hardness, chemical potential, electrophilicity index, and Mulliken charges. In comparison to the original chalcone **1**, all synthesized compounds **3–21** exhibited higher energy stability. Among them, compound **19** demonstrated a particularly high dipole moment, promoting the separation of charges and increasing reactivity. Meanwhile, compound **9** displayed higher hardness and lower softness values, displaying lower intramolecular charge transfer. Furthermore, compound **9** had the highest ΔE value, indicating greater kinetic stability, while compound **6b** had the lowest ΔE, indicating high chemical reactivity. The DFT calculations were also used to determine the molecular electrostatic potential (MEP) of the two compounds that demonstrated the highest antioxidant activity.

Conflicts of interest

The authors declare that they have no known competing financial interests or personal relationships that could have appeared to influence the work reported in this paper.

Acknowledgements

The Authors acknowledge the National research centre and Ain Shams University for the facilities provided.

References

1 A. Mermer, T. Keles and Y. Sirin, *Bioorg. Chem.*, 2021, **114**, 105076.
2 A. M. Fahim and M. A. Shalaby, *J. Mol. Struct.*, 2019, **1176**, 408–421.
3 A. I. Khodair, S. E. Kassab, N. A. Kheder and A. M. Fahim, *Carbohydr. Res.*, 2022, **514**, 108546.
4 A. M. Farag and A. M. Fahim, *J. Mol. Struct.*, 2019, **1179**, 304–314.
5 R. J. Obaid, N. Naeem, E. U. Mughal, M. M. Al-Rooqi, A. Sadiq, R. S. Jassas, Z. Moussa and S. A. Ahmed, *RSC Adv.*, 2022, **12**, 19764–19855.
6 A. M. Fahim, M. A. Shalaby and M. A. Ibrahim, *J. Mol. Struct.*, 2019, **1194**, 211–226.
7 S. A. Rizk, S. S. Abdelwahab and H. A. Sallam, *J. Heterocycl. Chem.*, 2018, **55**, 1604–1614.
8 M. A. Fahim, S. M. Elshikh and M. N. Darwish, *Curr. Comput.-Aided Drug Des.*, 2020, **16**, 486–499.
9 S. Wang, X.-H. Yuan, S.-Q. Wang, W. Zhao, X.-B. Chen and B. Yu, *Eur. J. Med. Chem.*, 2021, **214**, 113218.
10 P. Bhutani, G. Joshi, N. Raja, N. Bachhav, P. K. Rajanna, H. Bhutani, A. T. Paul and R. Kumar, *J. Med. Chem.*, 2021, **64**, 2339–2381.
11 P. Das, M. D. Delost, M. H. Qureshi, D. T. Smith and J. T. Njardarson, *J. Med. Chem.*, 2018, **62**, 4265–4311.
12 A. M. Fahim and E. H. Ismael, *Egypt. J. Chem.*, 2019, **62**, 1427–1440.
13 S. A. Rizk and S. Shaban, *J. Heterocycl. Chem.*, 2019, **56**(9), 2379–2388.
14 K. N. M. Halim, S. A. Rizk, M. A. El-Hashash and S. K. Ramadan, *J. Heterocycl. Chem.*, 2021, **58**, 636–645.
15 Y. U. Cebeci, H. Bayrak, Ş. A. Karaoğlu and A. M. Fahim, *J. Mol. Struct.*, 2022, **1260**, 132810.
16 S. A. Rizk, A. A. El-Sayed and M. M. Mounier, *J. Heterocycl. Chem.*, 2017, **54**, 3358–3371.
17 H. ur Rashid, M. A. U. Martines, A. P. Duarte, J. Jorge, S. Rasool, R. Muhammad, N. Ahmad and M. N. Umar, *RSC Adv.*, 2021, **11**, 6060–6098.
18 B. Colom-Fernández, A. Kreutzman, A. Marcos-Jiménez, V. García-Gutiérrez, C. Cuesta-Mateos, I. Portero-Sainz, Y. Pérez-García, L. F. Casado, F. Sánchez-Guijo and J. Martínez-López, *Front. Pharmacol.*, 2019, **10**, 1340.
19 F. C. K. Dolk, K. B. Pouwels, D. R. Smith, J. V. Robotham and T. Smieszek, *J. Antimicrob. Chemother.*, 2018, **73**, ii2–ii10.
20 K. Haider, M. Shafeeque, S. Yahya and M. S. Yar, *J. Med. Chem. Rep.*, 2022, 100042.
21 A. Kumar, A. K. Singh, H. Singh, V. Vijayan, D. Kumar, J. Naik, S. Thareja, J. P. Yadav, P. Pathak and M. J. P. Grishina, *Pharmaceuticals*, 2023, **16**, 299.
22 A. Aboelnaga, E. Mansour, A. M. Fahim and G. H. Elsayed, *J. Mol. Struct.*, 2022, **1251**, 131945.
23 A. M. Fahim, A. M. Farag, A. Mermer, H. Bayrak and Y. Şirin, *J. Mol. Struct.*, 2021, **1233**, 130092.
24 J. Cossy and A. Guerinot, in *Advances in Heterocyclic Chemistry*, Elsevier, 2016, vol. 119, pp. 107–142.
25 A. M. Fahim, H. E. M. Tolan and H. Awad, *J. Iran. Chem. Soc.*, 2021, **18**, 2965–2981.
26 S. Rizk, *Egypt. J. Chem.*, 2008, **51**, 611–621.
27 X. Wang, Q. Hu, H. Tang and X. Pan, *Pharmaceuticals*, 2023, **16**, 228.
28 M. Ashfaq, M. N. Tahir, K. S. Munawar, R. Behjatmanesh-Ardakani and H. Kargar, *J. Mol. Struct.*, 2022, **1261**, 132952.
29 B. Meyer, *Chem. Rev.*, 1976, **76**, 367–388.
30 R. Mehmood, E. U. Mughal, E. B. Elkaeed, R. J. Obaid, Y. Nazir, H. A. Al-Ghulikah, N. Naeem, M. M. Al-Rooqi, S. A. Ahmed and S. W. A. Shah, *ACS omega*, 2022, **7**, 30215–30232.
31 S. B. Nimse and D. Pal, *RSC Adv.*, 2015, **5**, 27986–28006.
32 A. Mermer and S. Alyar, *Chem.-Biol. Interact.*, 2022, **351**, 109742.
33 A. Gusain, N. Kumar, J. Kumar, G. Pandey and P. K. Hota, *J. Fluoresc.*, 2021, **31**, 51–61.
34 W. A. Yehye, N. A. Rahman, A. Ariffin, S. B. Abd Hamid, A. A. Alhadi, F. A. Kadir and M. Yaeghoobi, *Eur. J. Med. Chem.*, 2015, **101**, 295–312.

35 T. Jaehnert, M. D. Hager and U. S. Schubert, *J. Mater. Chem. A*, 2014, **2**, 15234–15251.
36 M. Carocho and I. C. Ferreira, *Food Chem. Toxicol.*, 2013, **51**, 15–25.
37 S. Schmidt and J. Pokorný, *Czech J. Food Sci.*, 2005, **23**, 93–102.
38 J. Hu, L. Yang, P. Yang, S. Jiang, X. Liu and Y. Li, *Biomater. Sci.*, 2020, **8**, 4940–4950.
39 C. Nopo-Olazabal, J. Hubstenberger, L. Nopo-Olazabal and F. Medina-Bolivar, *J. Agric. Food Chem.*, 2013, **61**, 11744–11758.
40 D. Charles, *Antioxidant Properties of Spices, Herbs and Other Sources*, Springer, New York, NY, 2012.
41 S. K. Ramadan and S. A. Rizk, *J. Iran. Chem. Soc.*, 2022, **19**, 187–201.
42 S. Upadhyay, A. C. Tripathi, S. Paliwal and S. K. Saraf, *Pharm. Chem. J.*, 2017, **51**, 564–575.
43 M. Shyam, H. Verma, G. Bhattacharje, P. Mukherjee, S. Singh, S. Kamilya, P. Jalani, S. Das, A. Dasgupta, A. Mondal, A. K. Das, A. Singh, F. Brucoli, C. Bagnéris, R. Dickman, V. N. Basavanakatti, P. Naresh Babu, V. Sankaran, A. Dev, B. N. Sinha, S. Bhakta and V. Jayaprakash, *J. Med. Chem.*, 2022, **65**, 234–256.
44 A. M Fahim, E. H. I. Ismael, G. H. Elsayed and A. M. Farag, *J. Biomol. Struct. Dyn.*, 2022, **40**(19), 9177–9193.
45 A. Nie, J. Wang and Z. Huang, *J. Comb. Chem.*, 2006, **8**, 646–648.
46 M. A. Shalaby, H. M. Al-Matar, A. M. Fahim and S. A. Rizk, *J. Phys. Chem. Solids*, 2022, **170**, 110933.
47 H. Loghmani-Khouzani, P. Tamjidi, I. Mohammadpoor-Baltork, M. Yaeghoobi, N. A. Rahman, A. R. Khosropour, M. Moghadam, S. Tangestaninejad, V. Mirkhani, M. H. Habibi, A. Kashima and T. Suzuki, *J. Heterocycl. Chem.*, 2014, **51**, 138–150.
48 S. Vilar, G. Cozza and S. Moro, *Curr. Top. Med. Chem.*, 2008, **8**, 1555–1572.
49 K. A. Hicks, S. E. O'Leary, T. P. Begley and S. E. Ealick, *Biochemistry*, 2013, **52**, 477–487.
50 G. H. Elsayed, S. Dacrory and A. M. Fahim, *Int. J. Biol. Macromol.*, 2022, **222**, 3077–3099.
51 P. Pyykkö, *Chem. Soc. Rev.*, 2008, **37**, 1967–1997.
52 M. Spiegel, T. Marino, M. Prejanò and N. Russo, *Phys. Chem. Chem. Phys.*, 2022, **24**, 16353–16359.
53 M. Spiegel, T. Marino, M. Prejanò and N. Russo, *J. Mol. Liq.*, 2022, **366**, 120343.
54 C. Peng, P. Y. Ayala, H. B. Schlegel and M. J. Frisch, *J. Comput. Chem.*, 1996, **17**, 49–56.
55 H. B. Schlegel, *J. Comput. Chem.*, 1982, **3**, 214–218.
56 A. Mohamed, A. M. Fahim and M. A. Ibrahim, *J. Mol. Model.*, 2020, **26**, 354.
57 G. Zhang and C. B. Musgrave, *J. Phys. Chem. A*, 2007, **111**, 1554–1561.
58 V. Choudhary, A. Bhatt, D. Dash and N. Sharma, *J. Comput. Chem.*, 2019, **40**, 2354–2363.
59 A. Nekrouf, K. Toubal, Y. Megrouss, N. E. H. Belkafouf, A. Djafri, N. Khelloul, J.-C. Daran, A. Djafri and A. Chouaih, *J. Mol. Struct.*, 2022, **1262**, 133002.
60 Z. Demircioğlu, G. Kaştaş, Ç. A. Kaştaş and R. Frank, *J. Mol. Struct.*, 2019, **1191**, 129–137.
61 J. Pandey, P. Prajapati, A. Srivastava, P. Tandon, K. Sinha, A. P. Ayala and A. K. Bansal, *Spectrochim. Acta, Part A*, 2018, **203**, 1–12.
62 A. M. Fahim, H. S. Magar and N. H. Mahmoud, *Appl. Organomet. Chem.*, 2023, **37**(4), e7023.
63 A. Attia, A. Aboelnaga and A. M. Fahim, *Egypt. J. Chem.*, 2022, DOI: **10.21608/ejchem.2022.166142.7046**.
64 B. M. Ivković, K. Nikolic, B. B. Ilić, Ž. S. Žižak, R. B. Novaković, O. A. Čudina and S. M. Vladimirov, *Eur. J. Med. Chem.*, 2013, **63**, 239–255.
65 M. Shyam, H. Verma, G. Bhattacharje, P. Mukherjee, S. Singh, S. Kamilya, P. Jalani, S. Das, A. Dasgupta and A. Mondal, *J. Med. Chem.*, 2022, **65**, 234–256.
66 A. M. A. Algohary, A. M. Hassan, A. Y. Alzahrani and S. A. Rizk, *J. Heterocycl. Chem.*, 2023, **1**, DOI: **10.1002/jhet.4647**.
67 M. A. Shalaby, A. M. Fahim and S. A. Rizk, *Sci. Rep.*, 2023, **13**, 4999.
68 R. Ramajayam, R. Giridhar, M. R. Yadav, H. Djaballah, D. Shum and C. Radu, *J. Enzyme Inhib. Med. Chem.*, 2007, **22**(6), 716–721.
69 A. M. Fahim, *J. Mol. Struct.*, 2023, **1277**, 134871.
70 K. M. Elokely and R. J. Doerksen, *J. Chem. Inf. Model.*, 2013, **53**, 1934–1945.
71 J. Cheeseman, G. Scalmani, V. Barone, B. Mennucci, G. Petersson, H. Nakatsuji, M. Caricato, X. Li, H. Hratchian and A. Izmaylov, *Gaussian 09, Revision A.02*, Inc., Wallingford, 2009.